PCCP

ON THE STABILITY OF MANGANESE TRIS (β-DIKETONATE) COMPLEXES AS REDOX MEDIATORS IN DSSCs

Journal:	*Physical Chemistry Chemical Physics*
Manuscript ID	CP-ART-09-2015-005524.R1
Article Type:	Paper
Date Submitted by the Author:	01-Dec-2015

Complete List of Authors:	Carli, Stefano; University of Ferrara, Chemistry Caramori, Stefano; University of Ferrara, Chemistry Argazzi, Roberto; ISOF-CNR, Bignozzi, C A; University of Ferrara, Chemistry Bernardi, Tatiana; University of Ferrara, Chemistry Bertolasi, Valerio; University of Ferrara, Chemistry Casarin, Laura; University of Ferrara, Chemistry Benazzi, Elisabetta; University of Ferrara, Chemistry

ON THE STABILITY OF MANGANESE *TRIS* (β-DIKETONATE) COMPLEXES AS REDOX MEDIATORS IN DSSCs.

Stefano Carli*,[a] Elisabetta Benazzi,[a] Laura Casarin,[a] Tatiana Bernardi,[a] Valerio Bertolasi,[a] Roberto Argazzi,[b] Stefano Caramori,[a] and Carlo Alberto Bignozzi*.[a]

(a) Department of Chemical and Pharmaceutical Sciences of the University of Ferrara, Via Fossato di Mortara 17-27, 44121, Ferrara, Italy

(b) CNR-ISOF c/o Department of Chemical and Pharmaceutical Sciences of the University of Ferrara, Via Fossato di Mortara 17-27, 44121, Ferrara, Italy

* crlsfn@unife.it

* g4s@unife.it

ABSTRACT

The photoelectrochemical properties and stability of dye sensitized solar cells containing Mn(β-diketonato)$_3$ complexes, [Mn^{III}(acac)$_3$] **(1)** (acac = acetylacetonate), [Mn^{III}(CF2)$_3$] **(2)** (CF2 = 4,4-difluoro-1-phenylbutanate-1,3-dione), [Mn^{III}(DBM)$_3$] **(3)** (DBM = dibenzoylmethanate), [Mn^{II}(CF2)$_3$]TBA (TBA = tetrabutylammonium) **(4)** and [Mn^{II}(DBM)$_3$]TBA **(5)**, have been evaluated. At room temperature, the complexes undergo ligand exchange with 4-tert-buthyl-pyridine, an additive commonly used in the solar device to reduce charge recombination at the photoanode. An increased device stability was achieved by using the Z907 dye and passivating the photoanode with short chain siloxanes. It was also found that the Mn(II)/(III) couple is involved in the dye regeneration process, instead of Mn(III)/(IV) ($E_{1/2}$ > 1V Vs SCE) previously indicated in the literature.

INTRODUCTION

Dye-sensitized solar cells (DSSCs) are essentially biphasic systems in which a mesoporous photoactive substrate (photoanode), usually composed of a wide band gap semiconductor sensitized by appropriate charge-transfer molecules, is in contact with either a liquid or a gel electrolyte containing ionic or molecular species acting as electron mediators which allow for hole transfer to a dark counter electrode.[1]

Since the initial reports,[1,2] most of the research and the industrialization efforts on DSSCs have considered the I_3^-/I^- redox couple as ideal candidate to balance the dual kinetic constraint of fast dye regeneration and slow charge recombination. However, regrettably, this redox couple has a list of undesirable chemical properties: first, the use of iodide based electrolytes results in a large voltage loss across the cell, due to the usually large overpotential for dye regeneration; I_2 in equilibrium with I_3^- is volatile, complicating long term cell sealing; I_3^- is darkly coloured limiting the light harvesting efficiency of the dye; I^-/I_3^- is corrosive and will corrode most metals, posing a serious problem to a long term protection of metallic conductors used to increase the efficiency of electron collection.[3,4] Starting from 2000 the search for alternative electron mediators has become an active field of research,[5,6] exploring the properties of redox tunable transition metal complexes based on Fe(III)/(II),[7,8] Co(III)/(II),[9,10] Ni(IV)/(III)[11] and Cu(II)/(I),[12,13] as well as on organic

molecules like TEMPO,[14] and thiolate/disulfide.[15] It was observed that when used in conjunction with specific dye architectures, some of these redox couples allowed to obtain considerably high solar cell efficiencies.[16-18]

Among the first row transition metals, manganese can be considered an interesting candidate for the variety of accessible redox states, its low toxicity and abundance. The first example of application was reported in 2014 by Spiccia et al, which focused on DSSCs containing the commercially available $[Mn(acac)_3]^{0/+1}$ (acac = acetylacetonate) and the MK2 dye, reporting an energy conversion efficiencies of 4.4%, under AM 1.5 G, 100 mW cm^{-2}.[19] Following that report we prepared a series of tris-(β-diketonato) manganese complexes, namely $[Mn^{III}(CF2)_3]$ **(2)** (CF2 = 4,4-difluoro-1-phenylbutanate-1,3-dione), $[Mn^{III}(DBM)_3]$ **(3)** (dbm = dibenzoylmethanate), $[Mn^{II}(CF2)_3]$TBA **(4)** and $[Mn^{II}(DBM)_3]$TBA **(5)** (TBA = tetrabutylammonium), comparing their properties to $[Mn^{III}(acac)_3]$ **(1)**. The study revealed that Mn(II)/(III) is the relevant redox couple involved in the dye regeneration process and that all species are unstable, at room temperature, with respect to ligand exchange with 4-tert-butyl-pyridine (TBP), an additive normally used to reduce charge recombination.[20]

RESULTS AND DISCUSSION

Synthesis

The Mn complexes object of this study are schematized in Figure 1, where **4** and **5** are the reduced form of **2** and **3**, respectively.

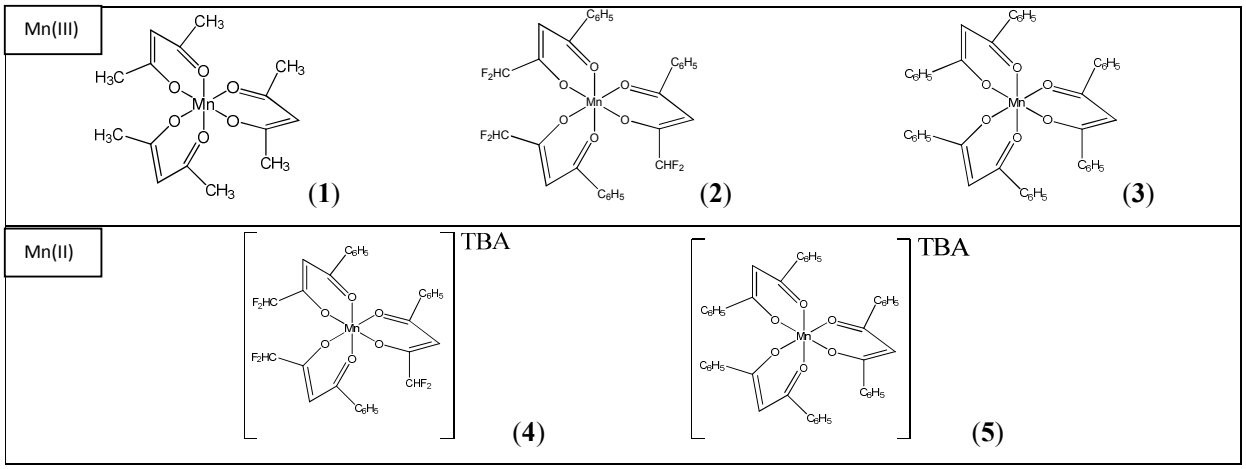

Figure 1. Tris-(β-diketonato) Mn complexes.

Tris-(β-diketonato) Mn(III) complexes are generally prepared by treatment of an aqueous solution of potassium permanganate with acetylacetone.[21-22] Attempts to prepare **2** and **3,** in high yields, with this method however failed and the two complexes were obtained by treating a solution of Mn(III) acetate with an excess of the respective ligand in hot toluene. The products were then isolated by crystallization in a

mixture of diethyl ether and pentane. The divalent manganese complexes **4** and **5** were prepared in high yields by reacting the appropriate ligand with a Mn^{II} precursor in methanol at room temperature. All products were characterized by ESI mass, UV/Vis spectroscopy and cyclic voltammetry. The *fac*-$[Mn(CF2)_3]$ **(2)** complex crystallizes in the trigonal *R-3* space group with the central Mn(III) on the crystallographic special position *3*. Therefore, the complex **2** displays a C_3 symmetry where the three equivalent CF2 ligands exhibit Mn1-O1 and Mn1-O2 distances of 1.978(2) and 1.995(2) Å, respectively (Figure 2, Tables S1a and S1b). Accordingly, the complex which shows a slight distorted octahedral geometry does not display the typical Jahn-Teller distorsion as observed for $[Mn(acac)_3]$[22] **(1)** and $[Mn(DBM)_3]$ **(3).**[23]

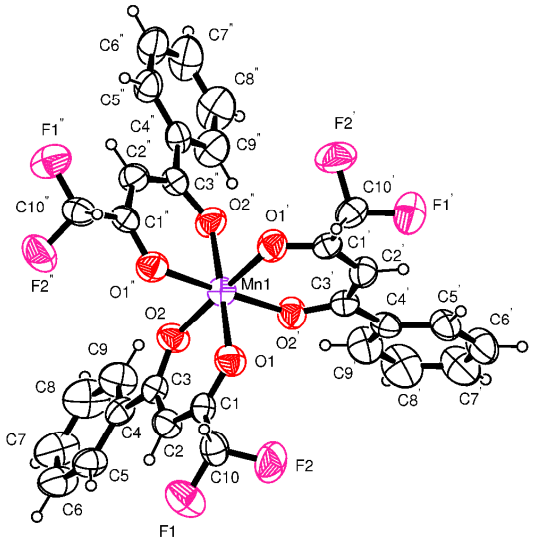

Figure 2. ORTEP drawing of **2**.

ESI mass

Mass characterization of $[Mn(acac)_3]$ **(1)** has previously been performed by electron ionization (EI),[24] matrix-assisted laser desorption/ionization time-of-flight mass spectrometry (MALDI-TOFMS),[25] and electrospray ESI[26]. Generally manganese(III) tris(acetylacetonato) exhibits the same dominant fragmentation, namely, the loss of a single ligand yielding the base peak $[Mn(acac)_2]^+$, unlike high pressure EI that can reveal molecular cation radical $[Mn(acac)_3]^{\bullet+}$ (usually of low abundance).[27] The ESI spectra of the commercial $[Mn(acac)_3]$ **(1)** is reported in Figure S1. As expected, the main peak is relative to $[Mn(acac)_2]^+$ (m/z = 253), but it can be observed a secondary peak at m/z = 294, related to the solvent-complex $[Mn(acac)_2ACN]^+$ (ACN = acetonitrile), the molecular cationic radical $[Mn(acac)_3]^{\bullet+}$ (m/z = 352) and the sodium adduct $[Mn(acac)_3 + Na]^+$ (m/z = 375). A similar fragmentation pattern was observed for **2**

and **3** (Figure S2, S3). ESI mass of Mn(II) complexes **4** and **5** were detected in negative ion mode, showing the molecular anions $[Mn(CF2)_3]^-$ and $[Mn(DBM)_3]^-$ as the most intense signals (Figure S4, S5).

Electronic Absorption Spectroscopy.

The electronic absorption spectra of Mn(III) and Mn(II) complexes (Figure S6), show the typical d-d transitions at wavelengths > 450 nm, with maximum molar extinction coefficients of ca 250 M^{-1} cm^{-1} for Mn (III)[28] and 400 M^{-1} cm^{-1} for Mn(II) species.

Electrochemistry

The electrochemistry of Mn complexes **1**,**2**,**3** has been studied by cyclic voltammetry (CV) in acetonitrile and overlaid CV plots and relevant electrochemical data are reported in Figure 3 and Table 1 respectively.

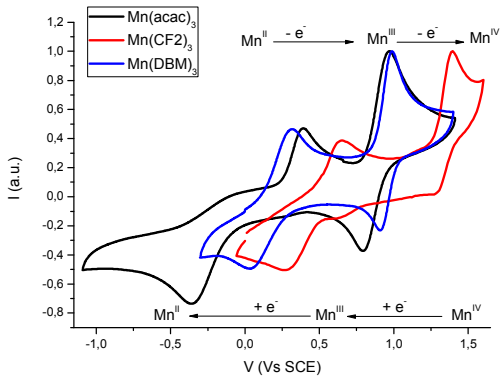

Figure 3. CV of $[Mn(acac)_3]$ **(1)**, $[Mn(CF2)_3]$ **(2)** and $[Mn(DBM)_3]$ **(3)** in 0.1M $LiClO_4$/ACN solution at 100 mV s^{-1} scan rate, glassy carbon WE, Pt wire CE.

All CVs are characterized by two redox waves corresponding to the oxidation of Mn(III) to Mn(IV), with $E_{1/2}$ in the range of +0.8 ÷ 1.4 V vs SCE, and to the reduction of Mn(III) to Mn(II) in the potential range of 0 ÷ -0. 5 V vs SCE (Figures 3).[29] The latter process is electrochemically irreversible showing a large peak splitting between reductive and oxidative processes, most probably consequence of the lack of ligand field stabilization for the high spin d^5 configuration of Mn(II) with consequent large inner sphere contribution to electron transfer, while the former is quasi-reversible.[29]

	$Mn^{II} \rightarrow Mn^{III}$				$Mn^{III} \rightarrow Mn^{IV}$			
	E_{pc} (V)	E_{pa} (V)	ΔE (mV)	$E_{1/2}$ (V)	E_{pc} (V)	E_{pa} (V)	ΔE (mV)	$E_{1/2}$ (V)
$[Mn(acac)_3]$**(1)**	-0.37	0.39	760	0.01	0.79	0.97	180	0.88
$[Mn(CF2)_3]$ **(2)**	0.26	0.64	380	0.45	1.28	1.39	110	1.33
$[Mn(DBM)_3]$ **(3)**	0.00	0.139	139	0.07	0.93	0.99	60	0.96

Table 1. Relevant data obtained from CV analysis of **1**[29-33], **2** and **3**[29] (potentials are referred to SCE).

Photoelectrochemistry

The JV plots of MK2[34] sensitized solar cells, containing [Mn(acac)$_3$] **(1)** and [Mn(CF2)$_3$] **(2)** as redox mediators, in ACN and MPN are reported in Figure 4. For stability tests, MPN was preferred because of its lower volatility. Complex [Mn(DBM)$_3$] **(3)**, was only slightly soluble in MPN, preventing the comparison with the other two mediators at concentration levels of the order of 0.15M. For these reasons, MK2 sensitized solar cells were only tested with the redox mediators **1** and **2**.

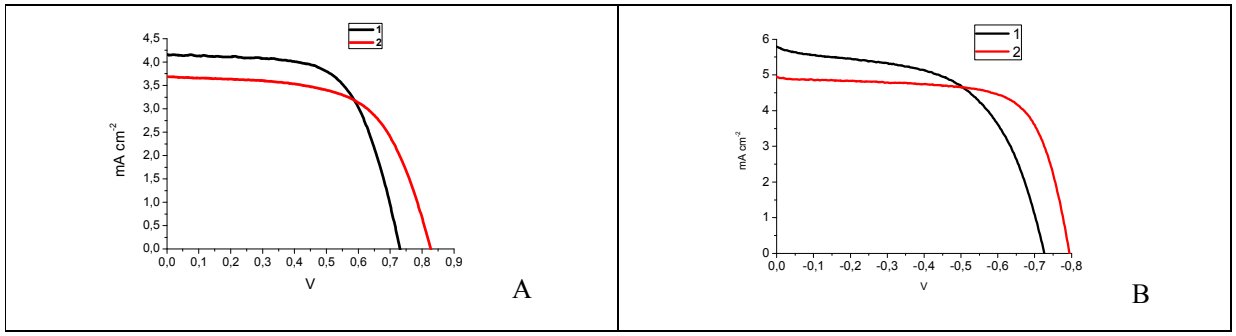

Figure 4. electrolyte composition: 0.15M **1** or **2** , 0.5M TBP, 0.1M LiCF$_3$SO$_3$, 0.015M NOBF$_4$ in A) MPN and B) ACN.

The higher performances observed in ACN (Figure 4B) are due to the lower solvent viscosity favoring the diffusional transport of the redox couple between the cell electrodes and within the pores of the TiO_2. In these experimental conditions, overall efficiencies η%, of the order of 1.55**(1)**, 1.89**(2)**, 2.36**(1)**, 2.72**(2)**, were obtained in MPN and ACN respectively. Corresponding short circuit photocurrents, open circuit photovoltages and fill factors are reported in Table S2. For comparison, MK2 sensitized DSSCs were also prepared with an optimized [Mn(acac)$_3$] **(1)** acetonitrile based electrolyte, and the results were consistent with previously reported data[19] (see Figure S7 and Table S3).

In general, depending on the dye, both redox couples Mn(II)/(III) and Mn(III)/(IV) can be involved in the regeneration processes. In conjunction with the MK2 dye, Spiccia et al [19] indicated Mn(III) as responsible for dye regeneration, this contrasts, however, with the thermodynamics of the bimolecular electron transfer process. ΔG values can be obtained from the redox potentials according to: $\Delta G = -ne[(E_{1/2}(D^+/D) - (E_{1/2}(M^{ox}/M^{red})]$, where *n* is the number of electrons transferred, *e* is the elemental charge of the electron, $E_{1/2}(D^+/D)$ and $E_{1/2}(M^{ox}/M^{red})$ are the redox potentials of the sensitizer and redox mediator, respectively. As reported in the electrochemical section, and supported by literature reports,[29-32] the redox potentials for the couples $[Mn^{III/IV}(acac)_3]^{0/+1}$, $[Mn^{III/IV}(CF2)_3]^{0/+1}$ and $[Mn^{III/IV}(DBM)_3]^{0/+1}$ are +1.12V, +1.57V and +1.20V (Vs NHE) respectively, with the dye exhibiting a reversible $[MK2]^{0/+1}$ process at +1.12V Vs NHE (Figure S8). Considering in addition the redox potential for MK2 adsorbed on TiO_2 , which spans from +0.89 V[35], +0.92 V[19] and +0.96 V[36] Vs NHE, it appears that the Mn(III)/(IV) redox couples cannot be involved in the

dye regeneration. From the redox potential (V, vs NHE) of the couples $[Mn^{II/III}(acac)_3]^{-1/0}$ (+0.24), $[Mn^{II/III}(CF2)_3]^{-1/0}$ (+0.69) and $[Mn^{II/III}(DBM)_3]^{-1/0}$ (0.41) driving forces for dye regeneration of 0.88 eV, 0.43 eV and 0.71 eV can be estimated, indicating that Mn(II) is the only species which can effectively reduce the oxidized MK2 dye during cell operation.

Electron Mediator Stability

4-tert-Butylpyridine (TBP) is one of the most useful additives for highly performing DSSC electrolytes, usually allowing for increased cell photovoltage and fill factor. Upon interaction of TBP with the TiO_2 surface, a negative shift of the semiconductor Fermi level and a decreased recombination rate between photoinjected electrons and the oxidized form of the electron mediator (dark current) occur.[37,38] This latter recombination process is important to the point that in the absence of photoanode passivation almost no photocurrent and photovoltage were detected in DSSCs containing Mn(III)/(IV) species. At the same time, in steady state irradiation experiments with the reported TBP containing electrolyte composition[19] in either ACN or MPN, we observed a considerable decay of the photoelectrochemical performances. Even in dark conditions at RT, solutions of Mn(II) or of Mn(III) complexes, in the presence of TBP, showed spectral changes indicating modifications of the solution composition, which in the case of **1** was almost complete after 48 h (Figure S9). In neat ACN no appreciable changes of the electronic absorption spectra were observed for **1**, **2, 3,** while for the reduced **4** and **5**, the spectral variations were consistent with oxidation to the corresponding Mn(III) species.

ESI mass spectra revealed that addition of TBP to $[Mn(acac)_3]$ **(1)** in ACN solution caused an almost immediate appearance of a new peak at m/z = 387 (Figure S10). Except for intensity variations, the ESI profile remained almost unchanged even after 24 hours with the most important peaks relative to the species $[Mn(acac)_2]^+$ m/z = 253, $[Mn(acac)_2ACN]^+$ m/z = 294 and to the species with m/z = 387 which best fit with a $[Mn(acac)_2TBP]^+$ fragmentation adduct. The ability of TBP in coordinating the Mn center was confirmed by X-ray structure on the crystals which spontaneously separated from the solution of ACN of **1** and **2** containing TBP. Figure 5 shows the structure of trans-$[Mn^{III}(acac)_2TBP_2]ClO_4$ and trans-$[Mn^{II}(CF2)_3TBP_2]^0$, where, in the latter case, the higher oxidation potential due to the fluorinated ligand, stabilizes Mn(II) in the complex; the corresponding crystallographic data are reported in Tables S4a,b and S5a,b.

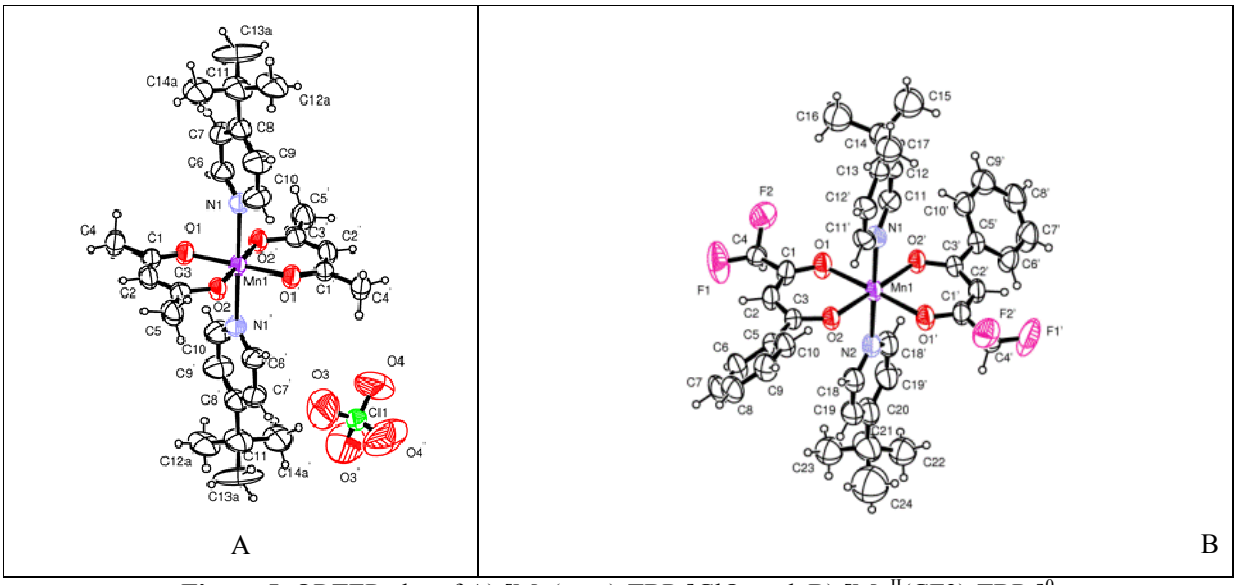

Figure 5. ORTEP plot of A) $[Mn(acac)_2TBP_2]ClO_4$ and B) $[Mn^{II}(CF2)_3TBP_2]^0$.

A similar behavior was observed for compound **3**, but in this case it was not possible to obtain crystals of the TBP containing complex. ESI profile confirms the same decomposition pattern observed for **1** and **2**, with the m/z = 636 which best fit with the $[Mn(DBM)_2TBP]^+$ fragmentation adduct (Figure S11). Attempts to use benzimidazole derivatives[39] led to similar electrolyte instability.

In order to improve the electrolyte stability and to suppress at the same time the dark current, without nitrogen based Lewis bases as TiO_2 passivating agents, we performed a series of experiments by using APTS silanized photoanodes[40], sensitized with the dye *cis*-$Ru(H_2dcbpy)(dnbpy)(NCS)_2$ (Z907, where the ligand H_2dcbpy is 4,4′-dicarboxylic acid-2,2′-bipyridine and dnbpy is 4,4′-dinonyl-2,2′-bipyridine), in the presence of the redox mediator **4** and **5** and of the corresponding oxidized forms **2** and **3**. Contrary to MK2, Z907 was found to exhibit a good adsorption stability following trialkoxysilane post-treatments of the sensitized photoanode[40,41] and was thus the dye considered for these studies. TiO_2 post functionalization with short chain siloxanes[39] was found to successfully screen the semiconductor surface from electron acceptors in the electrolyte by acting mainly through sterical blocking against neutral Mn(III) complexes. Sealed DSSCs showed an appreciable response, despite the absence of basic additives, reaching quickly the steady state under 1 sun and potential cycling at 10 mV/s (Figure 6), corresponding to overall efficiencies of 2.62% and 1.48% for $[Mn^{II/III}(CF2)_3]^{-1/0}$ and $[Mn^{II/III}(DBM)_3]^{-1/0}$ respectively (Figure 6, curves A,B). From Figure 6 it can be observed that the manganese series under investigations produce similar open circuit photovoltages despite variations in $E_{1/2}$ of the order of 400 mV ($E_{1/2}$ = 0.45 V vs SCE for $[Mn(CF_2)_3]$ **(2)** and 0.07 V vs SCE for $[Mn(DBM)_3]$ **(3)**). It can be observed that the Mn(III) mediators (Figure 6, curves C,D), also reach respectable efficiencies in the DSC based electrolytes, but such performances are only achieved after hundred cycles in LSV mode at 10 mv/s (Figure S12), necessary to accumulate Mn(II) by reduction of Mn(III) at the counter electrode of the cell. This corroborates the indication that Mn(II) is the active species

in the dye regeneration process in this type of manganese based electrolytes. 0.3 M Mn (II) approaches the solubility limit of the **4** and **5** species in the selected solvents (ACN, DMF/CAN 1/1). Tests carried out with 0.15 M Mn(II) resulted halved photocurrent densities with respect to the curves reported in figure 6 at least with acetonitrile solvent. On the other hand, the dependence of the photocurrent on the concentration is much less pronounced in the more viscous electrolytes containing DMF.

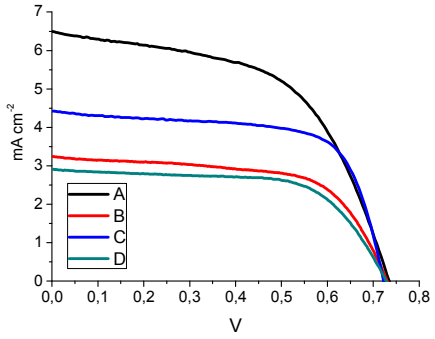

Figure 6. Z907/APTS sensitized DSC, electrolyte composition: A) 0.3/0.03M $[Mn^{II/III}(CF2)_3]^{-1/0}$ **(4)**, 0.1M $LiCF_3SO_3$, ACN; B) 0.3/0.03M $[Mn^{II/III}(DBM)_3]^{-1/0}$ **(5)**, 0.1M $LiCF_3SO_3$, ACN/DMF 1:1vol; C) 0.15M $[Mn^{III}(CF2)_3]^0$ **(2),** 0.1M $LiCF_3SO_3$, ACN; D) 0.13M $[Mn^{III}(DBM)_3]^0$ **(3)**, 0.1M $LiCF_3SO_3$, DMF.

The EIS investigation in the new Mn(II) electrolytes **5** and **4** outlines the higher charge transfer resistance of **5** (Figure 7A) compared to **4**. This indication is corroborated by the log R_{CT} vs log C_μ characteristic (Figure 7 C), where it can be observed that even at comparable chemical capacitance (i.e. density of occupied states) of the TiO_2 (ca. 2 10^{-4} F) the charge transfer resistance in the presence of **5** is about one order of magnitude larger than that observed in the presence of **4**. Further, the analysis of the log C_μ vs V_{TiO_2} behavior (figure 7 B) points out a substantial negative shift (ca. 300 mV) of the conduction band edge of the TiO_2 in the presence of **5**. These two effects provide a good explanation of the unexpectedly very similar open circuit voltages observed with the **5** and **4** redox couples, whose redox potential, i.e. the Fermi level of the counter electrode, differ by ca. 400 mV. In **5** the less positive potential is counterbalanced at the TiO_2/electrolyte interface by a slower electron recapture rate by Mn(III) and by a ca. 300 mV negative voltage offset of the lower conduction band edge. The more positive conduction band edge observed with the fluorinated manganese (II) mediator can be explained by the higher surface dipole induced by the interaction of the more polar **4** mediator with the semiconductor surface. We note that the lower photocurrent observed with **5** can be either ascribed to a reduction in the charge injection rate by the sensitizer, due to the decreased driving force following the negative shift of the conduction band edge, but also to a higher diffusional resistance, caused by the use of a more viscous electrolyte composed of a mixture of ACN and DMF, as can be appreciated by the large diffusional loop in Nyquist plots reported on the SI (Figure S13).

Finally, we point out that Z907 may not be the best dye to be used in conjunction with the investigated electron mediators. Sterically hindered organic dyes with a stable binding group in the presence of siloxane post treatments[42], having intense optical absorption, should allow the use of thinner TiO_2 layers, resulting in a further reduction of recombination events. The work is progressing toward this direction.

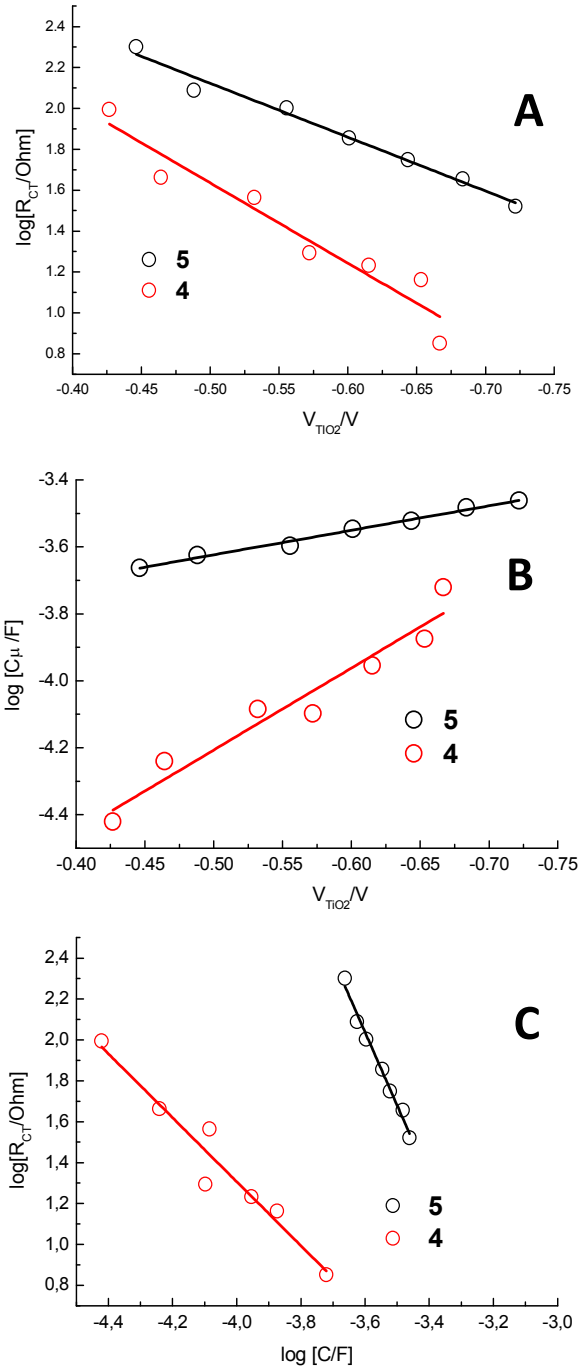

Figure 7. TiO_2 charge transfer resistance (R_{CT}) and chemical capacitance (C_μ) extracted from EIS under illumination. (A) log R_{CT} vs V_{TiO2}; (B) log C_μ vs V_{TiO2}; (C) log R_{CT} vs log C_μ

CONCLUSIONS

This study indicates that tris(β-diketonate)Mn complexes can operate with reasonable efficiency only in the presence of basic additives like TBP, tasked to the suppression of charge recombination at the TiO_2/electrolyte interface. However, under these conditions these Mn redox mediators are chemically unstable due to coordination of the basic nitrogen, leading to the formation *trans*-TBP substituted derivatives, as demonstrated by the crystal structure of the reaction products. In order to obtain solar devices with an increased stability, the presence of basic additives was avoided and TiO_2 passivation was achieved by co-adsorption of short chain siloxanes, acting as steric barrier against electron recapture by oxidized manganese species. Finally, the combined analysis of the electrochemical and photoelectrochemical properties revealed that Mn(II)/(III) is the redox couple involved in the dye regeneration process. To date, the results obtained with tris(β-diketonate)Mn complexes are still unsatisfactory with respect to other alternative metal based redox mediators, but it can be foreseen that the use of sterically hindered dyes, compatible with an appropriate photoanode passivation and TiO_2 optimization may lead to better DSSC performances which will also allow a deeper understanding of the charge transfer dynamics involving this new class of redox relays.

EXPERIMENTAL SECTION

Materials. All chemicals were Sigma Aldrich products and were used as received. Conductive FTO (fluorine tin oxide) TEC8, 2.3 mm thick substrates (Pilkington) were carefully cleaned by several washings in ethanol, acetone, and Alconox followed by annealing at 400 °C in air before use. TiO_2 colloidal paste (DSC 18NRT) was purchased from Dyesol. Mass spectrometry was performed in ESI mode with a Finningan LCQ Duo Ion Trap (Capillary Temp: 250 °C, Infusion flow rate: 18 μL/min, Sheath gas flow rate: 20 AU), or with a Waters Micromass ZQ 2000 (Cone Temperature 110°C and desolvation Temperature of 130°C, Capillary voltage 2.30 KV, Cone Voltage 20 V, Extractor Voltage 3V and RF Lens Voltage 0.3V, Flow rate 295 L/hr) under positive/negative mode acquisition. Cyclic Voltammetry plots were collected in a standard three-electrode cell with an Autolab PGSTAT 302/N potentiostat at a scan rate of 100 mV s^{-1} with a standard calomel electrode as reference, a Pt wire as auxiliary, and a glassy carbon as working electrode. Absorption spectra were collected with a JASCO V 570 UV–Vis spectrophotometer.

Synthesis of Mn(III) complexes. A stirred solution of $Mn(CH_3COO)_3 \times 2H_2O$ (200 mg, 0.74 mmol) in toluene (25 mL) was treated with an excess of the ligand (CF2 or DBM) (4.93 mmol). The mixture was heated under stirring for 6 hours, cooled to room temperature and the solvent was removed with a rotavapor. The residue was dissolved in the minimum amount of diethyl ether and n-exane was added until a green to

brown solid separated. After several hours the precipitate was filtrated under vacuum and washed several times with n-exane. Yields in the range of 50÷60%. $[Mn(CF2)_3]$ **(2).** m/z (ESI): 449 $[Mn(CF2)_2]^+$ calculated for $C_{30}H_{21}F_6MnO_6$ 646.2. ε_{560} (M cm^{-1}): 216. $[Mn(DBM)_3]$ **(3).** m/z (ESI): 501 $[Mn(DBM)_2]^+$ calculated for $C_{45}H_{33}MnO_6$ 724.2. ε_{560} (M cm^{-1}): 170.

Synthesis of $[Mn(CF2)_3]$TBA (4). A stirred solution of $Mn(CH_3COO)_2\times4H_2O$ (1 mmol) in methanol (25 mL) and $TBAPF_6$ (1 mmol) was treated, at room temperature, with a solution of CF2 (3 mmol) in the minimum amount of methanol. The yellow/orange solid was separated by filtration under vacuum and washed several times with cold methanol. Yields in the order of 50%. m/z (ESI): 646 $[Mn(CF2)_3]^-$ calculated for $C_{30}H_{21}F_6MnO_6$ 646.2. ε_{450} (M cm^{-1}): 370.

Synthesis of $[Mn(DBM)_3]$TBA (5). DBM (3 mmol) was added to a stirred solution of TBAOH (3 mmol, 30% mol in methanol) in methanol (25 mL). The stirred solution was treated, at room temperature, with $MnCl_2\times6H_2O$ (1 mmol) dissolved in the minimum amount of methanol. The yellow/orange solid was separated by filtration under vacuum and washed several times with cold methanol. Yields were in the order of 60%. m/z (ESI): 724 $[Mn(DBM)_3]^-$ calculated for $C_{45}H_{33}MnO_6$ 724.2. ε_{450} (M cm^{-1}): 273.

Solar Cell Fabrication. Mesoporous titania films (ca. 6 μm thick) were prepared by blading a commercial colloidal TiO_2 paste on FTO electrodes, which were left to dry under a gentle warm air stream before sintering at 450 °C for 30 min. The resulting transparent films were immersed in a 0.4 M $TiCl_4$ solution for 12 hours, rinsed with water and gradually heated at 500°C for 10 minutes. Finally, the photoanodes were immersed in a 0.2 mM solution of MK2 in a 1:1 toluene/acetonitrile mixture, or in a 0.3mM solution of Z907 in ethanol for 24 hours at room temperature. The silanization of Z907 sensitized photoanodes was performed as described in reference 40. Solar cells were assembled by holding the two electrodes together with metallic clamps and by using a 25 μm thick Surlyn frame as spacer. PEDOT based counter electrodes was prepared by potentiostatic anodic electropolymerization of 3,4-ethylenedioxythiophene (EDOT) on FTO glasses.[43]

Electrolyte Formulation. The electrolyte composition consisted of 0.15M **1** or **2** , 0.5M TBP, 0.1M $LiCF_3SO_3$, 0.015M $NOBF_4$ in a) MPN and b) ACN for JV shown in Figure 3, and A) 0.3/0.03M $[Mn^{II/III}(CF2)_3]^{-1/0}$ **(4)**, 0.1M $LiCF_3SO_3$, ACN; B) 0.3/0.03M $[Mn^{II/III}(DBM)_3]^{-1/0}$ **(5)**, 0.1M $LiCF_3SO_3$, ACN/DMF 1:1vol; C) $[Mn^{III}(CF2)_3]^0$ **(2)** 0.15M, 0.1M $LiCF_3SO_3$, ACN; $[Mn^{III}(DBM)_3]^0$ **(3)** 0.13M, 0.1M $LiCF_3SO_3$, DMF for JV shown in Figure 6.

Solar Cell Characterization. Current−voltage measurements were performed with an Autolab PGSTAT 302/N potentiostat at a scan rate of 20 mV s^{-1}. Cell performances were evaluated under AM 1.5G illumination (ABET sun simulator). Electrochemical impedance spectroscopy (EIS) of **5** and **4** mediated solar cells under AM 1.5G was recorded with an Autolab PGSTAT 302/N potentiostat by using a 10 mV sinusoidal perturbation in the 10^5–10^{-2} Hz frequency range. The DC potential was sampled along the ascending branch of the JV curve with an interval of 20 mV starting from Voc. Impedance data were analyzed using commercially available Z-View software and were fitted with the simplified equivalent electric circuit reported in Scheme 1, where the R2-CPE1 mesh describes the TiO_2/electrolyte

electrochemical interface, W_s represents the short Warburg diffusion element and R3-CPE2 stands for the counter electrode/electrolyte interface. The non ideal capacitances of the electrochemical interfaces are described by constant phase elements (CPE) with exponents in the range 0.95±0.05. Ws is the short Warburg element describing electrolyte diffusion in a thin layer cell. Typical maximum errors from fits were <10 %.

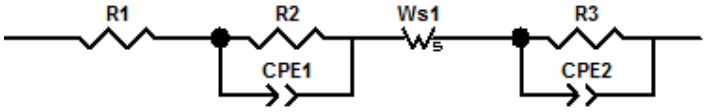

Scheme 1: electric model used to fit experimental EIS data at open circuit.

TiO_2 charge transfer and chemical capacitance where plotted against the voltage drop occurring at the TiO_2 interface (V_{TiO2}) calculated by $V_{TiO2} = V_{app}-iR_S$ and $Rs = R_\Omega + R_{CE} + R_D$ where R_Ω, R_{CE} and R_D are the ohmic, counter electrode charge transfer and diffusional resistances respectively and I is the photocurrent recorded at the given voltage V_{app}

Stability test. Stability tests were carried out in acetonitrile solutions containing 0.1 M $LiClO_4$ and a 0.15 M concentration of the selected Mn complex, either $[Mn(acac)_3]$ **(1) or** $[Mn(CF2)_3]$ **(2)**. In the case of $[Mn(DBM)_3)]$ **(3) (**0.13 M) DMF/0.1 M $LiClO_4$ was used. Each solution was treated with an excess of TBP (3.3 equivalents). The resulting solutions were stored in the dark at room temperature. Spectra were recorded by diluting the mother solutions with acetonitrile to a nominal final concentration of 1.2×10^{-4} M of the initial Mn complex.

Crystallization of complexes. Dark-green crystals of **2** were obtained by slow evaporation of the solvent from a 0.15M solution in ACN. Yellow/orange crystals spontaneously separated by the electrolyte solution after two weeks or 24 hours for *trans*-$[Mn^{III}(acac)_2TBP_2]ClO_4$ and *trans*-$[Mn^{II}(CF2)_3TBP_2]^0$ respectively.

Crystallography. The crystal data of compounds *fac*-$[Mn(CF2)_3]$**(2)**, *trans*-$[Mn^{III}(acac)_2TBP_2]ClO_4$ and *trans*-$[Mn^{II}(CF2)_3TBP_2]^0$ were collected at room temperature using a Nonius Kappa CCD diffractometer with graphite monochromated Mo-Kα radiation. The data sets were integrated with the Denzo-SMN package[44] and corrected for Lorentz, polarization and absorption effects (SORTAV)[45]. The structures were solved by direct methods using SIR97[46] system of programs and refined using full-matrix least-squares with all non-hydrogen atoms anisotropically and hydrogens included on calculated positions, riding on their carrier atoms. All calculations were performed using SHELXL-97[47] and PARST[48] implemented in WINGX[49] system of programs. The Figures have been drawn using the program ORTEP[50]. The crystal data are given in the Supporting Material.

Crystallographic data have been deposited at the Cambridge Crystallographic Data Centre and allocated the deposition numbers CCDC1421029-1421030-1421031. These data can be obtained free of charge via

www.ccdc.cam.ac.uk/conts/retrieving.html or on application to CCDC, Union Road, Cambridge, CB2 1EZ, UK [fax: (+44)1223-336033, e-mail: deposit@ccdc.cam.ac.uk]

NOTES AND REFERENCES

(1) O'Regan, B.; Graetzel, M. *Nature* **1991**, *353*, 737−740.
(2) Hagfeldt, A.; Graetzel, M. *Acc. Chem. Res.* **2000**, *33*, 269.
(3) Nusbaumer, H.; Zakeeruddin, S. M.; Moser, J. E.; Graetzel, M. *Chem. Eur. J.* **2003**, *9*, 3756.
(4) Toivola, M.; Ahlskog, F.; Lund, P. *Sol. Energ. Mat. Sol. Cells* **2006**, *90*, 2881.
(5) Wu, J.; Lan, Z.; Lin, J.; Huang, M.; Huang, Y.; Fan, L.; Luo, G. *Chem. Rev.* **2015**, *115*, 2136−2173.
(6) Bignozzi, C. A.; Argazzi, R.; Boaretto, R.; Busatto, E.; Carli, S.; Ronconi, F.; Caramori, S. *Coord. Chem. Rev.* **2012**, *257*, 1472.
(7) Caramori, S.; Husson, J.; Beley, M.; Bignozzi, C. A.; Argazzi, R.; Gros, P. C. *Chem. Eur. J.* **2010**, *16*, 2611−2618.
(8) Gregg, B. A.; Pichot, F.; Ferrere, S.; Fields, C. L. *J. Phys. Chem. B* **2001**, *105*, 1422.
(9) Sapp, S. A.; Elliott, C. M.; Contado, C.; Caramori, S.; Bignozzi, C. A. *J. Am. Chem. Soc.* **2002**, *124*, 11215−11222.
(10) Nusbaumer, H.; Moser, J. E.; Zakeeruddin , S. M.; Nazeeruddin, M. K.; Graetzel, M. *J. Phys. Chem. B* **2001**, *105*, 10461−10464.
(11) Li, T. C.; Spokoyny, A. M.; She, C.; Farha, O. K.; Mirkin, C. A.; Marks, T. J.; Hupp, T. J. *J. Am. Chem. Soc.* **2010**, *132*, 4580−4582.
(12) Hattori, S. W., Y.; Yanagida, S.; Fukuzumi, S. *J. Am. Chem. Soc.* **2005**, *127*, 9648−9654.
(13) Bai, Y.; Yu, Q.; Cai, N.; Wang, Y.; Zhang, M.; Wang, P. *Chem. Commun.* **2011**, *47*, 4376−4378.
(14) Zhang, Z.; Chen, P.; Murakami, T. N.; Zakeeruddin, S. M.; Graetzel, M. *Adv. Funct. Mater.* **2008**, *18*, 341−346.
(15) Wang, M.; Chamberland, N.; Breau, L.; Moser, J. E.; Humphry-Baker, R.; Marsan, B.; Zakeeruddin, S. M.; Graetzel, M. *Nat. Chem.* **2010**, *2*, 385−389.
(16) Feldt, S. M.; Gibson, E. A.; Gabrielsson, E.; Sun, L.; Boschloo, G.; Hagfeldt, A. *J. Am. Chem. Soc.* **2010**, *132*, 16714−16724.
(17) Daeneke, T.; Kwon, T. H.; Holmes, A. B.; Duffy, N. W.; Bach, U.; Spiccia, L. *Nat. Chem.* **2011**, *3*, 211−215.
(18) Tsao , H. N.; Yi , C.; Moehl, T.; Yum, J. H.; Zakeeruddin, S. M.; Nazeeruddin, M. K.; Graetzel, M. *ChemSusChem* **2011**, *4*, 591
(19) Perera, I. R.; Gupta, A.; Xiang, W.; Daeneke, T.; Bach, U.; Evans, R. A.; Ohlin, C. A.; Spiccia, L. *Phys. Chem. Chem. Phys.* **2014**, *16*, 12021.
(20) Nazeeruddin, M. K.; Kay, A.; Rodicio, I.; Humpbry-Baker, R.; Miiller, E.; Liska, P.; Vlachopoulos, N.; Gratzel, M. *J. Am. Chem. Soc.* **1993**, *115*, 6382.
(21) Bhattacharjee, M. N.; Chaudhuri, M. K.; Khathing, D. T. *Journal of the Chemical Society, Dalton Transactions* **1982**, 669.
(22) Geremia, S.; Demitri, N. *J. Chem. Educ.* **2005**, *82* 460.
(23) Freitag, R.; Muller, T. J.; Conradie, J. *J. Chem. Crystallogr.* **2014**, *45*, 352.
(24) Bancroft, G. M.; Reichert, C.; Westmore, J. B. *Inorg. Chem.* **1968**, *7*, 870.
(25) Wyatt, M. F.; Havard, S.; Stein, B. K.; Brenton, A. G. *Rapid Commun. Mass Spectrom.* **2008**, *22*, 11.

(26) Henderson W., M. J. S. *Mass Spectrometry of Inorganic and Organometallic Compounds: Tools - Techniques – Tips*; John Wiley & Sons, 2005.
(27) Schildcrout, S. M. *J. Phys. Chem.* **1976**, *80*, 2834.
(28) Barnum, D. W. *J. Inorg. Nucl. Chem.* **1961**, *21*, 221.
(29) Freitag, R.; Conradie, J. *Electrochim. Acta* **2015**, *158* 418.
(30) Pacześniak, T.; Błoniarz, P.; Rydel, K.; Sobkowiak, A. *Electroanalysis* **2007** *9*, 945.
(31) Bond, A. M.; Martin, R. I.; Master, s. A. F. *Inorg. Chem.* **1975** *14*, 1432.
(32) Richert, S. A.; Tsang, P. K. S.; Sawyer, D. T. *Inorg. Chem.* **1989** *28* 2471.
(33) Gritzner, G.; Murauer, H.; Gutmann, V. *J. Electroanal. Chem.* **1979**, *101*, 185.
(34) Koumura, N.; Wang, Z. S.; Mori, S.; Miyashita, M.; Suzuki, E.; Hara, K. *J. Am. Chem. Soc.* **2006**, *128*, 14256.
(35) Daeneke, T.; Mozer, A. J.; Uemura, Y.; Makuta, S.; Fekete, M.; Tachibana, Y.; Koumura, N.; Bach, U.; Spiccia, L. *J. Am. Chem. Soc.* **2012**, *134*, 16925.
(36) Wang Z. S., K. N., Cui Y., Takahashi M., Sekiguchi H., Mori A., Kubo T., Furube A., Kohjiro H. *Chem. Mater.* **2008**, *20*, 3993.
(37) Nazeeruddin M. K., K. A., Rodicio I., Humpbry-Baker R., Miiller E., Liska P., Vlachopoulos N., Gratzel M. *J. Am. Chem. Soc.* **1993**, *115*, 6382.
(38) Koh, T. M.; Nonomura, K.; Mathews, N.; Hagfeldt, A.; Grätzel, M.; Mhaisalkar, S. G.; Grimsdale, A. C. *J. Phys. Chem. C* **2013**, *117*, 15515−15522.
(39) Kusama, H.; Arakawa, H. *J. Photochem. Photobiol. A* **2004**, *162*, 441.
(40) Carli, S.; Casarin, L.; Caramori, S.; Boaretto, R.; Busatto, E.; Argazzi, R.; Bignozzi, C. A. *Polyhedron* **2014**, *82*, 173.
(41) Mba, M.; D'Acunzo, M.; Salice, P.; Maggini, M.; Caramori, S.; Campana, A.; Aliprandi, A.; Argazzi, R.; Carli, S.; Bignozzi, C. A. *J. Phys. Chem. C* **2013**, *117*, 19885−19896.
(42) Kakiage, K.; Aoyama, Y.; Yano, T.; Otsuka, T.; Kyomen, T.; Unno, M.; Hanaya, M. *Chem. Commun.* **2014**, *50*, 6379.
(43) Carli, S.; Busatto, E.; Caramori, S.; Boaretto, R.; Argazzi, R.; Timpson, C. J.; Bignozzi, C. A. *J. Phys. Chem. C* **2013**, *117*, 5142−5153.
(44) Otwinowski, Z.; Minor, W. *Methods in Enzymology (Macromolecular Crystallography Part A)* **1997**, *276*, 307.
(45) Blessing, R. H. *Acta Crystallogr. Sect A* **1995**, *51*, 33.
(46) Altomare, A. B., M. C.; Camalli,M.; Cascarano, G. L.; Giacovazzo, C.; Guagliardi, A.; Moliterni, A. G.; Polidori G.; Spagna, R. *J. Appl. Crystallogr.* **1999**, *32*, 115.
(47) Sheldrick, G. M. *Program for Crystal Structure Refinement, University of Gottingen, Germany* **1997**.
(48) Nardelli, M. *J. Appl. Crystallogr.* **1995**, *28*, 659.
(49) Farrugia, L. J. *J. Appl. Crystallogr.* **1999**, *32*, 837.
(50) Burnett M. N.; Johnson, C. K. *ORTEP III, Report ORNL-6895, Oak Ridge National Laboratory, Oak Ridge, TN* **1996**.